Lab on a Chip

PAPER

View Article Online
View Journal

Cite this: DOI: 10.1039/d0lc00304b

Smartphone-based multiplex 30-minute nucleic acid test of live virus from nasal swab extract†

Fu Sun, [a] Anurup Ganguli, [b] Judy Nguyen,[c] Ryan Brisbin,[d] Krithika Shanmugam,[d] David L. Hirschberg,[cd] Matthew B. Wheeler, [e] Rashid Bashir, [ab] David M. Nash[f] and Brian T. Cunningham*[ab]

Received 25th March 2020,
Accepted 17th April 2020

DOI: 10.1039/d0lc00304b

rsc.li/loc

Rapid, sensitive and specific detection and reporting of infectious pathogens is important for patient management and epidemic surveillance. We demonstrated a point-of-care system integrated with a smartphone for detecting live virus from nasal swab media, using a panel of equine respiratory infectious diseases as a model system for corresponding human diseases such as COVID-19. Specific nucleic acid sequences of five pathogens were amplified by loop-mediated isothermal amplification on a microfluidic chip and detected at the end of reactions by the smartphone. Pathogen-spiked horse nasal swab samples were correctly diagnosed using our system, with a limit of detection comparable to that of the traditional lab-based test, polymerase chain reaction, with results achieved in ~30 minutes.

Introduction

Since the SARS-CoV-2 (COVID-19) virus jumped from an animal reservoir to humans in December 2019, it has rapidly spread across the world, bringing death, illness, disruption to daily life, and economic losses to businesses and individuals. A key failure of the health system across every country has been the ability to rapidly and accurately diagnose the disease, with contributing factors that include a limited number of available test kits, a limited number of certified testing facilities, combined with the length of time required to obtain a result and provide information to the patient. The challenges associated with rapid diagnostic testing contribute to uncertainty surrounding which individuals should be quarantined, sparse epidemiological information, and inability to quickly trace pathogen transmission within/across communities. The challenges underlying COVID-19 diagnosis are already well known from previous encounters with emerging epidemics and pandemics, such as mosquito-borne diseases (zika, dengue, chikungunya, malaria), HIV, and others. Already, the ability to perform pervasive testing has shown clear benefits to countries that implement it, such as South Korea, to provide accurate information regarding whom to quarantine, which in turn results in more timely control of disease propagation.

Infectious diseases represent a global challenge for both human and animal health due to their ability to proliferate rapidly through direct or indirect contact, insect vectors, and respiratory inhalation.[1,2] Although the world's leading causes of human mortality are shifting toward non-communicable diseases, infectious diseases still accounted for 8.14 million deaths in 2017. This represented about 14.6% of total global deaths, which is comparable to the number of deaths caused by all cancers.[3] Infectious disease transmission within animal populations raised for food consumption result in substantial economic loss and is an ongoing threat to food production, as highlighted by a recent outbreak.[4] Additionally, animal populations kept for companion, racing or entertainment purposes are comprised of individuals with large sentimental or economic value, for which rapid point-of-care diagnostic tests would be particularly valuable. The availability of such tests would help guide treatment decisions or determine the necessity of quarantine. The issues facing human and animal transmission of respiratory diseases are very similar in terms of collection of samples by nasal swab, laboratory-based assays using polymerase chain reaction (PCR), and interventions that suppress disease spread such as quarantine and distancing from others.

A 2011 outbreak of equine herpesvirus type 1 (EHV1) originated from an American horse competition and rapidly

[a] Department of Electrical and Computer Engineering, University of Illinois at Urbana-Champaign, Illinois, USA. E-mail: bcunning@illinois.edu; Fax: +1 217 244 6375; Tel: +1 217 333 2301
[b] Department of Bioengineering, University of Illinois at Urbana-Champaign, Illinois, USA
[c] RAIN Incubator, Tacoma, Washington, USA
[d] Department of Interdisciplinary Arts and Sciences & The Center for Urban Waters, University of Washington Tacoma, Washington, USA
[e] Department of Animal Sciences, University of Illinois at Urbana-Champaign, Illinois, USA
[f] Private equine veterinarian, Kentucky, USA

† Electronic supplementary information (ESI) available. See DOI: 10.1039/d0lc00304b

spread to at least 242 horse premises in 19 U.S. states, with further spread to two Canadian provinces.[5] Due to shared living facilities, shared water sources, and physical contact with humans, the threat of equine infectious diseases is ever-present.[6–8] Effective equine infection surveillance and control should incorporate early-stage diagnosis to facilitate early medical intervention, and provide timely alerts that can contain outbreaks locally.[9]

Presently, a variety of diagnostic methods are available that can detect and identify infectious diseases, including direct microscopic examination, isolation of pathogens in culture, serological tests of antibody response, and nucleic acid testing (NAT) such as PCR assays.[10,11] Traditional diagnostic methods generally require benchtop instruments handled by trained personnel in a lab within a central facility. While sample preparation and the assay protocol may only require a few hours, the time delay imposed by sample delivery, along with timing uncertainty induced by testing backlogs, holidays, and other scheduled laboratory closures can cause a significant delay of results to the veterinarian. Furthermore, because many infectious diseases present themselves with similar symptoms and there is also a possibility of co-infection with more than one pathogen, the need to perform multiple tests to identify potential pathogens can cause further delays. An improved capability for pathogen testing would therefore be the ability to specifically identify multiple pathogens with a single test. Because available technologies remain expensive (in terms of capital equipment and reagents), technically challenging, and labor intensive, there is an urgent need for low-cost portable platforms that can provide fast, accurate, and multiplex diagnosis of infectious disease at the point of care.

In the area of human infectious disease testing, well-equipped laboratories are generally remotely located from low-income, resource-limited areas.[12] To meet the diagnostic needs of low-resource settings, point-of-care (POC) assay technology platforms have been developed to provide rapid, inexpensive and portable solutions.[13–15] NATs represent an important class of POC technologies for pathogen sensing that achieve a high level of specificity through detection of a nucleic acid sequence that has been carefully selected to identify only one pathogen species. In addition to high specificity, many NATs are capable of achieving high sensitivity through the use of enzymatic amplification of the target nucleic acid sequence. A single pathogenic DNA sequence can be converted into large numbers of copies that optionally carry fluorometric or colorimetric tags. Due to their success in laboratory settings, considerable efforts have been devoted to performing NATs in POC settings, with methods based upon PCR among the most prevalent.[16–18] The enzymatic amplification process inherent with PCR requires repeated heating/cooling cycles, resulting in detection systems with elaborate thermal control schemes that contribute to increased cost and complexity. Therefore, NATs that utilize isothermal nucleic acid amplification[19,20] have been investigated for implementing simple and miniaturized POC devices. Loop-mediated isothermal amplification (LAMP) is one such method that amplifies DNA at a constant temperature (60 to 65 °C) with only one type of enzyme and four to six primers.[21,22] This method can generate 10^9 copies of a specific target sequence in less than an hour. While LAMP primer design is more complex than PCR primer design, the LAMP process is generally considered less susceptible to the presence of materials that inhibit PCR and can operate in unprocessed samples such as cell lysate. Thus, LAMP-based NATs for identification of pathogens has been pursued for POC applications using dedicated readout instruments that detect fluorescent amplicons in both macrofluidic[23,24] and microfluidic[25,26] formats.

Recent research has consistently demonstrated that the image sensors integrated within commercially available smartphones have sufficient sensitivity for detecting fluorescence in the contexts of fluorescence microscopy of cells,[27] viruses,[28] and bacteria.[29] Smartphone cameras are likewise capable of sensing the fluorescent emission from a wide variety of biological assays,[30,31] including LAMP, within microfluidic compartments.[25,26,32] The advantage of using a smartphone as the detection instrument for POC analysis is that, it is possible to take advantage of the integrated optics, image sensor, computation power, user interface, and wireless communication capabilities of mobile devices, thus minimizing cost. With assistance from an inexpensive snap-in cradle or clip-on instrument, anyone that carries a smartphone would have the ability to perform testing. Due to the prevalence of cloud-based service systems, one can envision systems that integrate testing results from large numbers of users over a geographically distributed area for reporting of new infections and for epidemiological analysis of disease spread.

In this work, we used a portable smartphone-based instrument to perform end-point fluorescence detection of LAMP assays on a microfluidic chip for five bacterial and viral pathogens that cause equine respiratory infectious diseases and are most prevalent among horse populations: *Streptococcus equi* subspecies equi (*S. equi*), *Streptococcus equi* subspecies zooepidemicus (*S. zoo*), equine herpesvirus 1 (EHV1), equine herpesvirus 4 (EHV4) and equine influenza virus (EIV) subtype H3N8. A qualitative detection threshold was established after statistical analysis of positive and negative test values. Our system can detect the specific target nucleic acid sequences in a multiplex manner without signal crosstalk. Moreover, horse nasal swab samples spiked with one of the virus targets (EHV1) were tested by our system to demonstrate its capability in early-stage diagnosis. This work represents, to our knowledge, the first utilization of smartphone-based LAMP detection of pathogens for POC application in animal health. Utilizing the system in the context of equine respiratory diseases represents a model system for human pathogens such as SARS-CoV-2, which does not pose biosafety issues, but preserves the main features of a human COVID-19 testing protocol. Although our system was used to detect pathogenic DNAs in this paper for

demonstration, it can be easily adapted for detecting RNA viruses by using a one-step RT-LAMP protocol which adds reverse transcriptase to the LAMP reaction mix without modification to the buffer or reaction conditions.

Experimental

LAMP assays

LAMP assays were developed for specific nucleic acid sequences of the five equine pathogens. Another two LAMP assays detecting nucleic acid sequences within the genomes of *Escherichia coli* (*E. coli*) and equine herpesvirus 3 (EHV3) were used as positive controls for on-chip tests. A set of scrambled primers that had no target nucleic acid sequence among our test samples was a negative control. The primers (Tables S1 and S2†) of these LAMP assays were synthesized by Integrated DNA Technologies.

The LAMP assays were comprised of the following components (Table S3†): 1.4 mM of deoxynucleoside triphosphates (dNTPs), 1× isothermal amplification buffer (New England Biolabs), 6 mM of $MgSO_4$ (New England Biolabs), 0.4 M of betaine (Sigma-Aldrich), 640 units per mL Bst 2.0 WarmStart DNA Polymerase (New England Biolabs), 1× EvaGreen dye (Biotium), and a LAMP primer mix of 0.2 μM of F3 and B3 primers, 1.6 μM of FIP and BIP primers, and 0.8 μM of LoopF and LoopB primers. To make a 20 μL final reaction mix, 6.4 μL of template DNA and 1.8 μL of DEPC-treated water (Invitrogen) was added. The components were prepared in bulk and stored at −20 °C before reactions were prepared on ice.

Target template sequences were synthesized and cloned in the pUC57-AMP vector (Genewiz). Cultures of transformed *E. coli* were grown overnight and used to extract plasmids. The concentrations of plasmids were quantified using a Qubit Fluorometer (Invitrogen) and converted to a copy number using the plasmid's length.

Off-chip LAMP assays were carried out in 0.2 mL PCR reaction tubes, each with 10 μL of reaction mix, in an Eppendorf Mastercycler Real-Time PCR System. The tubes were incubated at 65 °C for 60 min in the thermocycler and fluorescence data was recorded every minute.

PCR assay

The PCR assay for EHV1 was used for DNA quantification in clinical samples as a gold standard. The PCR standard curve of EHV1 DNA was established using synthesized EHV1 plasmid at log concentrations (Fig. S4†). The 20 μL PCR reaction mix consisted of the following components (Table S4†): 1× Luna Universal qPCR Master Mix (New England Biolabs), 5 μL of template DNA, 4 μL of nuclease-free water, and 0.25 μM of forward and reverse PCR primers.

Off-chip PCR tests were conducted on the same thermocycler with the following protocol using its fast ramp speed: 1 min of initial DNA denaturation at 95 °C, followed by 45 cycles of 95 °C (15 s of denaturation) and 60 °C (30 s of extension). Fluorescence data was recorded after each cycle.

Horse nasal swab samples

Six healthy adult horses used in this study were from horse farms in Champaign, IL, United States. Sterile rayon nasal swabs (OSOM, SEKISUI-185, Sekisui Diagnostics, Lexington, MA) were placed 1–2 cm into the nares of each horse to collect nasal secretions and/or mucus. Each individual swab with sample was then placed back in its sterile protective cover and transported to the lab at 4 °C. Each swab was then incubated in 2 mL of phosphate-buffered saline (PBS) solution (Thermo Fisher Scientific) at 4 °C overnight to release nucleic acids. The EHV1 virus stock (USDA 040-EDV) held at −80 °C was thawed and spiked into three of the six sample solutions at different dilutions (1 : 10, 1 : 100, 1 : 1000) to make three EHV1-positive samples representing high, moderate and low levels of EHV1 viral load, respectively. We had to make positive samples in this way because all the horses we had access to were healthy. For DNA extraction, 200 μL of nasal swab solution was processed by a high-throughput purification kit (QIAamp DNA Mini Kit, QIAGEN), with a final elution volume of 100 μL.

The purified solutions from the swab samples were tested by real-time PCR described above (Fig. S5†), and the concentration of EHV1 DNA in each solution (Table S5†) was calculated using the previously established PCR standard curve. The DNA concentrations (5.5×10^4 to 6.3×10^6 copies per mL) of the purified solutions from the positive swab samples are in the clinical range of EHV1 infection, which is reported to be above 10^5 copies per mL within 6 days post infection and above 10^4 copies per mL within 12 days post infection in nasal swab solution.[33]

Silicon chip for assays

Silicon microfluidic chips were used to hold LAMP assays as they are highly stable, have no auto-fluorescence and can be manufactured efficiently. The chips (25 mm × 15 mm × 0.5 mm) contained ten parallel flow channels (10 mm × 0.5 mm × 0.2 mm) with a volume of 1 μL each and all sharing the same inlet. The surface of the chip was thermally oxidized to grow a 200 nm layer of SiO_2 that served to reduce the potential for bare silicon to inhibit the amplification process. Full details about fabrication of the chip can be found in our previous publication.[32]

On-chip amplification

For on-chip tests, primers were deposited into the microfluidic channels by pipetting and allowed to dry (Fig. 1a). The primers were reconstituted into solution during the following addition of LAMP reaction mix. The desired pathogen panel is "programmed" into the chip by the deposition of specific primers in each channel. For example, in the multiplex tests for all five pathogens, channel 1 was the first positive control with the primers for the *E. coli* DNA. In order to assure that channel 1 provided a positive response, ~40 pg of the *E. coli* DNA is a component of the reaction mix. Channel 2 served as a second positive control

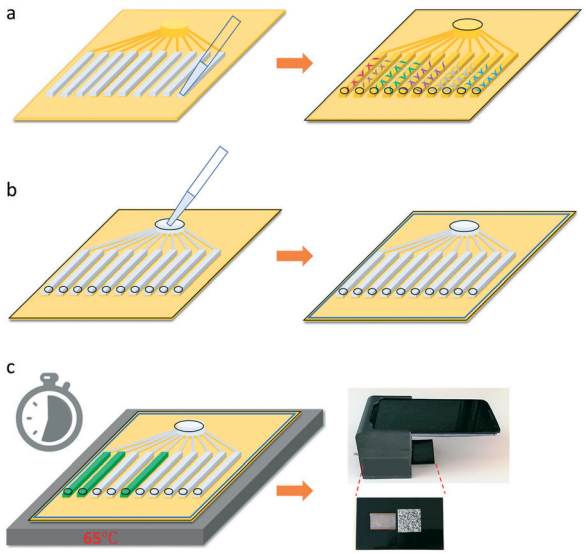

Fig. 1 On-chip detection workflow. a) Deposit controls and target primers into channels on a cleaned chip and cover it with a transparent double-side adhesive after reagents are dried; b) inject LAMP reaction mix from the inlet and seal the chip with a piece of cover glass; c) heat the chip at 65 °C for LAMP reactions and insert the chip into the cradle for end-point fluorescence imaging. Typically, results can be retrieved after 30 minutes.

by drying down a mixture of the primers and template DNA (1000 copies) for EHV3. Channel 3 was used as a negative control deposited with scrambled primers for goldfish DNA that should have no amplification for any pathogenic DNA sequence in our panel. The remaining channels were deposited with primers for pathogenic target sequences or left empty as needed. The primer solutions injected into the channels result in a final primer concentration the same as that used for off-chip LAMP assays. After deposition, the channels were covered with a layer of double-sided adhesive (DSA) and sealed by a piece of cover glass after sample injection (Fig. 1b) to prevent sample evaporation. The chip was then heated on a hotplate at 65 °C to drive the LAMP enzymatic amplification reactions (Fig. 1c).

Fluorescence image capture and analysis

Fluorescence images of amplified chips were captured using the rear-facing camera of a smartphone (Motorola Nexus 6) mounted on a custom-designed cradle.[32] The chip was illuminated with light from an array of eight blue LEDs (485 nm, #XPEBBL, Cree Inc.) arranged around the perimeter of the chip. The light from each LED was filtered by a small short pass optical filter (490 nm, #ZVS0510; Asahi Spectra) placed directly in front of it. A long pass optical filter (525 nm, #84-744; Edmund Optics) placed in front of a macro lens (12.5×, #TECHO-LENS-01, TECHO) allowed only the fluorescence emission of the EvaGreen DNA-intercalating dye to reach the camera. During image collection, the chip was heated to a temperature of ~65 °C by a positive temperature coefficient (PTC) heater (12 V–80 °C, Uxcell) in the cradle. The LED module and the heater were controlled by two separate switches on the cradle body. The LEDs were powered by two AAA batteries (3 V) and the heater was powered by a 9 V battery. A customized Android app was used for imaging with fixed settings (flashlight off, exposure time = 1 s). The app exported raw images. Each pixel within each image file was described by a three-dimensional matrix in red, green, blue (RGB) color space. The RGB intensity component for each pixel was stored as an 8-bit unsigned integer ranging from 0 to 255. The fluorescence emission from the Evagreen dye has a center wavelength of 533 nm, which falls within the spectral range of the green (G) channel, and thus only the G channel is used for the analysis. Within each microfluidic channel's region of interest in the image field of view, the average value of all the pixels were calculated. The average intensity obtained from the EHV3 positive control with 1000 copies of DNA was used for intensity normalization (value = 100) of all the channel intensities within the same chip.

Results and discussion

Determination of qualitative detection threshold

To identify the most suitable threshold intensity value to differentiate positive from negative tests, average intensities of positive and negative channels after LAMP reactions were collected for the EHV1 target DNA for concentrations ranging from 100 to 10 000 copies per μL (Fig. 2a). The results of the other four targets in on-chip experiments were shown in Fig. S2.† Among the ten channels on each chip, two of them were used for controls, and the other eight channels acted as replicates for a target. As the target DNA concentration increases, the distribution of the positive values moves to a higher level and has a smaller variation (Fig. 2b). The

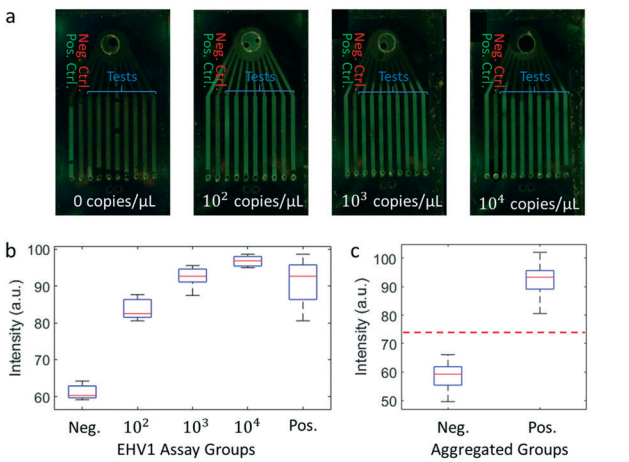

Fig. 2 On-chip characterization of the equine assays using plasmid DNA. a) Amplified chips with EHV1 templates at different concentrations (reagents dried on the chips from left to right in the image above for channel 1: positive control, channel 2: negative control, channel 3–10: EHV1 primers); b) the boxplots of average channel intensities of the above EHV1 samples; c) the boxplots of the overall negative and positive groups of five test assays, with the qualitative threshold marked by a red dash line.

negative channels with unamplified primers exhibit a low level of background fluorescence due to the presence of the intercalating dye. There is a distinct separation between the positive and negative intensity values (Fig. 2c). Based on the principle of support vector machine (SVM), the center value (threshold ≈ 74) between the lowest positive value and highest negative value was chosen as our positive/negative threshold, from which the distance to the nearest data points in the two groups is maximized.

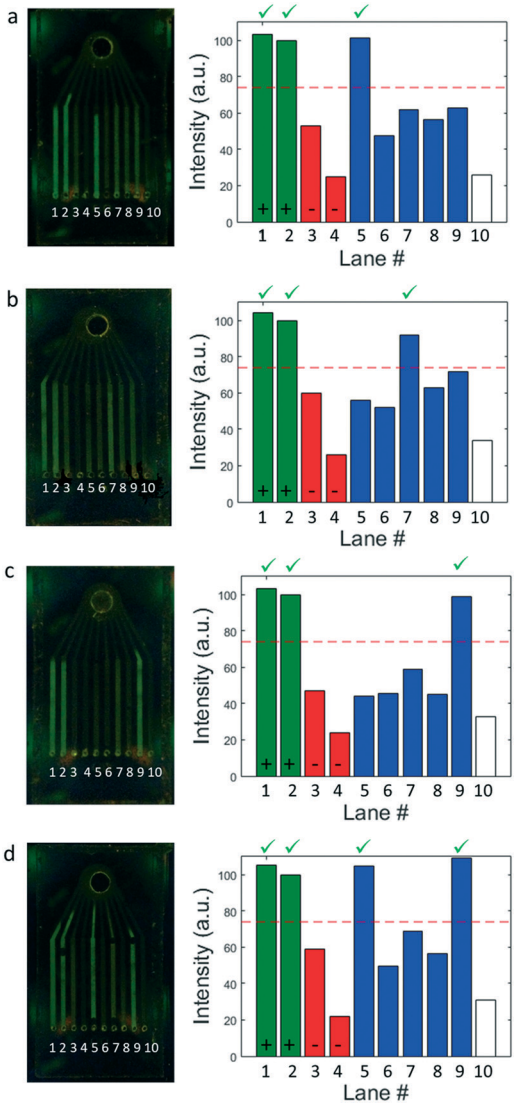

Fig. 3 On-chip multiplex detection of equine respiratory infection pathogen DNA. The smartphone images of amplified chips and the corresponding channel intensities are shown for detecting a) *S. equi*, b) EHV1, c) EIV and d) *S. equi* accompanied with EIV at 1000 copies per μL (reagents dried on the chip for channel 1: the *E. coli* positive control primers, channel 2: the EHV3 positive control primers and DNA, channel 3: the negative control primers, channel 4 and 10: no primers, channel 5–9: *S. equi*, *S. zoo*, EHV1, EHV4 and EIV primers, respectively. Green bars represent positive controls, red bars are for negative controls, and blue bars for tests. Channel 10 was an unused test channel, hence its signal was depicted as a white bar).

On-chip multiplex detection of pathogen DNA

Fig. 3 and S3† show smartphone images of the chips after amplification and corresponding average intensities in each channel. For multiplex detection of the five targets, channels 1–2 were used as positive controls as described previously, with target sequences integrated within the LAMP reaction mix (channel 1) or dried on the chip (channel 2) before sample injection, respectively. Both positive control channels

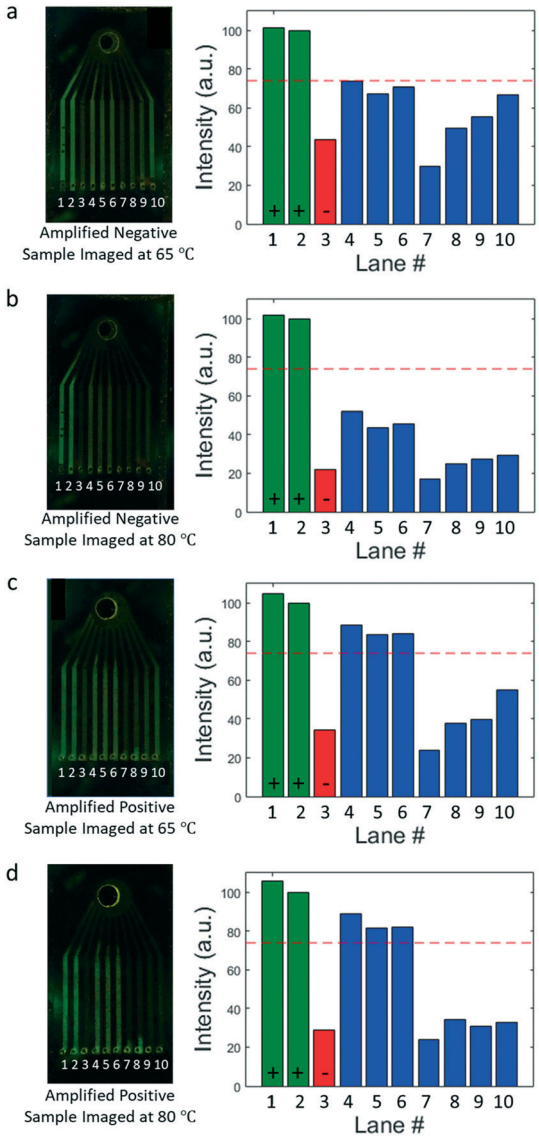

Fig. 4 On-chip tests of horse swab samples. The smartphone pictures were taken at a) 65 °C and b) 80 °C of the amplified chip for a negative sample and corresponding average channel intensities were analysed. The results for a positive sample (~5.48 × 10^4 EHV1 genome copies per mL) were also imaged at c) 65 °C and d) 80 °C. Increasing chip temperature at the imaging time decreased background fluorescence that may result from primer dimers and improved positive/negative contrast (reagents dried on the chip for channel 1: the *E. coli* positive control primers, channel 2: the EHV3 positive control primers and DNA, channel 3: the negative control primers, channel 4–6: EHV1 primers, channel 7–10: *S. equi*, *S. zoo*, EHV4 and EIV primers, respectively).

displayed strong fluorescence, indicating successful amplification that can also be used as references. Channel 3 contained primers used as a negative control. When comparing channel 3 and other unamplified reactions to channels containing no primers at all (channel 4 and 10), there were low levels of autofluorescence present. It was presumed that the background fluorescence was due to the binding of the dye with primers. After LAMP reactions, only the positive controls and the channel with the primers of the specific target in the sample passed the qualitative threshold. Minor to no evaporation of liquid was observed in channels after amplification and had no effect upon the qualitative positive/negative determination of a reaction. As shown in Fig. 3, the shared inlet and the majority of the linking channels between the inlet and individual channels remained dark, indicating no cross-contamination between channels. Because each of the LAMP reaction occurred independently within its microfluidic channel, the chip can also be used to detect coinfection with more than one pathogen (Fig. 3d).

On-chip tests of horse nasal swab samples

The processed horse nasal swab samples were tested on the chips with a new test layout: channels 1–2 were again utilized as positive controls, channel 3 was the negative control, channels 4–6 were prepared with the EHV1 primers as three replicates for the EHV1 assay, and channels 7–10 were utilized for the remaining four targets without replicates. Fig. 4 shows the results for a negative sample (Fig. 4a and b) and the lowest-concentration (5.5×10^4 copies per mL) positive sample (Fig. 4c and d). Our threshold was able to correctly classify all the positive and negative samples (the other samples in Fig. S6–S9†). We also found that taking end-point pictures of chips at a higher temperature after 65 °C amplification, for example, at 80 °C, would decrease the background fluorescence from negative channels and have little influence on positive channels, which provided improved overall contrast. We hypothesize that higher temperature prohibits formation of primer dimers that can bind to the EvaGreen dye and produce background fluorescence.

Conclusions

In summary, this study has demonstrated a smartphone-based system for rapid and multiplex detection of specific nucleic acids of five pathogens that cause equine respiratory infectious diseases. LAMP reactions were performed on a microfluidic chip with a reaction volume of 1 μL for each assay, and fluorescence images of the chips were taken by a smartphone in a customized cradle after isothermal LAMP amplification reaction. The microfluidic chip can be programmed for different target pathogens and sensing scenarios by changing the primer sets deposited in each channel. The integration of multiple positive/negative experimental controls and experimental replicates is used to assure that the assay protocol was performed correctly and can be used to reduce the likelihood of false positive or false negative results in POC health diagnostic applications. Our system is able to detect one or more specific targets simultaneously, which is valuable for coinfection diagnosis. The sensitivity of the system is adequate for early-stage detection of EHV1 in horse nasal swab samples, down to 5.5×10^4 copies per mL, which corresponds to about 18 copies per reaction and is comparable to the limit of detection of a PCR assay run on a commercial thermocycler. LAMP reactions take less than 30 minutes for high-concentration samples and the whole detection process can be finished in an hour with inexpensive and portable equipment, enabling veterinarians or physicians to diagnose infections at the point of care and report outbreaks remotely for efficient epidemic surveillance.

Our efforts are motivated by the urgent need to develop rapid POC testing for highly contagious human respiratory viruses such as SARS-CoV-2, that would enable results to be provided to the patient and physician as early as possible. By using a smartphone in conjunction with a cradle that enables the phone's camera to quickly gather a fluorescent endpoint image of the LAMP reaction, a positive/negative determination can be made that incorporates integrated experimental controls and replicates to assure that the test was performed correctly. By using the mobile device as a detection instrument, we envision that data collection can be seamlessly integrated with telemedicine platforms that facilitate epidemiology reporting and sharing test results with a physician. In future work, our plans include integrating the functions of viral lysis, LAMP buffer mixing, and LAMP reaction into a single cartridge with the reagents held within on-cartridge reservoirs. Further, we envision a detection instrument that clips onto a smartphone, with mechanical adapters that will align the rear-facing camera correctly with several popular phone models.

Author contribution

F. Sun, D. L. Hirschberg, R. Bashir and B. T. Cunningham conceived the idea and designed the study. F. S. designed, performed the experiments and wrote the manuscript. A. Ganguli provided the positive control assay. J. Nguyen designed the negative control primers. R. Brisbin prepared the quantified plasmids. K. Shanmugam helped J. Nguyen with off-chip experiments. D. M. Nash suggested the list of target equine pathogens. M. B. Wheeler provided the horse nasal swab samples. All offered intellectual inputs.

Conflicts of interest

Intellectual property associated with the technology described in this manuscript has been licensed by the University of Illinois to Reliant Immune Diagnostics (Austin, TX), where B. T. Cunningham serves as a consultant and owns stock options in the company.

Acknowledgements

The authors are grateful for the funding support provided by National Science Foundation (NSF) under the grant number 1534126. Any opinions, findings, and conclusions in this work are those of the authors and do not necessarily reflect the views of NSF.

Notes and references

1 A. J. Tatem, D. J. Rogers and S. I. Hay, *Adv. Parasitol.*, 2006, **62**, 293–343.
2 F. Fadel, M. Khalil El Karoui and B. Knebelmann, *Nat. Rev. Immunol.*, 2008, **8**, 153–160.
3 G. A. Roth, D. Abate, K. H. Abate, S. M. Abay, C. Abbafati, N. Abbasi, H. Abbastabar, F. Abd-Allah, J. Abdela and A. Abdelalim, *Lancet*, 2018, **392**, 1736–1788.
4 L. Reiley, A terrible pandemic is killing pigs around the world, and U.S. pork producers fear they could be hit next, https://www.washingtonpost.com/business/2019/10/16/terrible-pandemic-is-killing-pigs-around-world-us-pork-producers-fear-they-could-be-next/, (accessed Jan. 28, 2019).
5 J. Traub-Dargatz, A. Pelzel-McCluskey, L. Creekmore, S. Geiser-Novotny, T. Kasari, A. Wiedenheft, E. Bush and K. Bjork, *J. Vet. Intern. Med.*, 2013, **27**, 339–346.
6 S. Medić, S. Lazić, T. Petrović, D. Petrić, M. Samojlović, G. Lazić and D. Lupulović, *Acta Vet.*, 2019, **69**, 123–130.
7 A. Z. Durrani, M. Husnain, I. Haq, U. Batool and F. Khan, *2019 16th International Bhurban Conference on Applied Sciences and Technology (IBCAST)*, 2019, pp. 268–272, https://ieeexplore.ieee.org/document/8667229.
8 Defra, Animal Health Trust (AHT) and British Equine Veterinary Association, *Vet. Rec.*, 2019, vol. 184, pp. 761–765, https://veterinaryrecord.bmj.com/content/184/25/761.
9 L. Steele, E. Orefuwa and P. Dickmann, *Int. J. Infect. Dis.*, 2016, **53**, 15–20.
10 R. L. Kradin, *Diagnostic Pathology of Infectious Disease E-Book*, Elsevier Health Sciences, 2017.
11 D. C. Sellon and M. Long, *Equine Infectious Diseases*, Elsevier Health Sciences, 2013.
12 A. Prüss-Ustün, J. Bartram, T. Clasen, J. M. Colford Jr, O. Cumming, V. Curtis, S. Bonjour, A. D. Dangour, J. De France and L. Fewtrell, *Trop. Med. Int. Health*, 2014, **19**, 894–905.
13 P. Yager, G. J. Domingo and J. Gerdes, *Annu. Rev. Biomed. Eng.*, 2008, **10**, 107–144.
14 S. Sharma, J. Zapatero-Rodríguez, P. Estrela and R. O'Kennedy, *Biosensors*, 2015, **5**, 577–601.
15 S. Nayak, N. R. Blumenfeld, T. Laksanasopin and S. K. Sia, *Anal. Chem.*, 2016, **89**, 102–123.
16 A. Niemz, T. M. Ferguson and D. S. Boyle, *Trends Biotechnol.*, 2011, **29**, 240–250.
17 L. Zhang, B. Ding, Q. Chen, Q. Feng, L. Lin and J. Sun, *TrAC, Trends Anal. Chem.*, 2017, **94**, 106–116.
18 M. G. Mauk, J. Song, C. Liu and H. H. Bau, *Biosensors*, 2018, **8**, 17.
19 P. Gill and A. Ghaemi, *Nucleosides, Nucleotides Nucleic Acids*, 2008, **27**, 224–243.
20 Y. Zhao, F. Chen, Q. Li, L. Wang and C. Fan, *Chem. Rev.*, 2015, **115**, 12491–12545.
21 N. Tomita, Y. Mori, H. Kanda and T. Notomi, *Nat. Protoc.*, 2008, **3**, 877.
22 T. Notomi, H. Okayama, H. Masubuchi, T. Yonekawa, K. Watanabe, N. Amino and T. Hase, *Nucleic Acids Res.*, 2000, **28**, e63.
23 X. Ou, Q. Li, H. Xia, Y. Pang, S. Wang, B. Zhao, Y. Song, Y. Zhou, Y. Zheng and Z. Zhang, *PLoS One*, 2014, **9**, e94544.
24 A. Priye, S. W. Bird, Y. K. Light, C. S. Ball, O. A. Negrete and R. J. Meagher, *Sci. Rep.*, 2017, **7**, 1–11.
25 A. Ganguli, A. Ornob, H. Yu, G. Damhorst, W. Chen, F. Sun, A. Bhuiya, B. Cunningham and R. Bashir, *Biomed. Microdevices*, 2017, **19**, 73.
26 N. G. Schoepp, T. S. Schlappi, M. S. Curtis, S. S. Butkovich, S. Miller, R. M. Humphries and R. F. Ismagilov, *Sci. Transl. Med.*, 2017, **9**, eaal3693.
27 S. Knowlton, I. Sencan, Y. Aytar, J. Khoory, M. Heeney, I. Ghiran and S. Tasoglu, *Sci. Rep.*, 2015, **5**, 15022.
28 Q. Wei, H. Qi, W. Luo, D. Tseng, S. J. Ki, Z. Wan, Z. N. Göröcs, L. A. Bentolila, T.-T. Wu and R. Sun, *ACS Nano*, 2013, **7**, 9147–9155.
29 S. C. Gopinath, T.-H. Tang, Y. Chen, M. Citartan and T. Lakshmipriya, *Biosens. Bioelectron.*, 2014, **60**, 332–342.
30 H. Yu, Y. Tan and B. T. Cunningham, *Anal. Chem.*, 2014, **86**, 8805–8813.
31 D. Zhang and Q. Liu, *Biosens. Bioelectron.*, 2016, **75**, 273–284.
32 W. Chen, H. Yu, F. Sun, A. Ornob, R. Brisbin, A. Ganguli, V. Vemuri, P. Strzebonski, G. Cui and K. J. Allen, *Anal. Chem.*, 2017, **89**, 11219–11226.
33 G. A. Perkins, L. B. Goodman, E. J. Dubovi, S. G. Kim and N. Osterrieder, *J. Vet. Intern. Med.*, 2008, **22**, 1234–1238.